0022-3565/06/3171-1–10$20.00
THE JOURNAL OF PHARMACOLOGY AND EXPERIMENTAL THERAPEUTICS
JPET 317:1–10, 2006

Vol. 317, No. 1
96255/3085940
Printed in U.S.A.

Induction of Adenosine A_1 Receptor Expression by Pertussis Toxin via an Adenosine 5′-Diphosphate Ribosylation-Independent Pathway

Sarvesh Jajoo, Debashree Mukherjea, Sandeep Pingle, Yuko Sekino, and Vickram Ramkumar

Department of Pharmacology, Southern Illinois University School of Medicine, Springfield, Illinois (S.J., D.M., V.R.); Department of Pharmacology, Georgetown University, Washington, DC (S.P.); and Gunma University School of Medicine, Maebashi, Japan (Y.S.)

Received September 26, 2005; accepted November 30, 2005

ABSTRACT

Pertussis toxin ADP ribosylates G_i and G_o transducing proteins and functionally uncouples adenosine A_1 receptor (A_1AR) from its effectors. We hypothesized that this loss in receptor coupling could lead to de novo A_1AR synthesis by the cell in a futile attempt to re-establish normal receptor function. To test this hypothesis, we used hamster ductus deferens tumor (DDT_1 MF-2) cells, a cell culture model for studying A_1AR, and showed that pertussis toxin (100 ng/ml) produced a time-dependent loss in A_1AR-G_i interaction and abolished A_1AR activation of extracellular signal-regulated kinase 1/2. Interestingly, pertussis toxin increased the expression of A_1AR, as measured by real-time polymerase chain reaction, immunocytochemistry, and [^{3}H]cyclopentyl-1,3-dipropylxanthine (DPCPX) binding, suggesting a compensatory response to G_i protein inactivation. DDT_1 MF-2 cells exposed to pertussis toxin demonstrated nuclear factor κB (NF-κB) activation within 30 min of exposure, a time point that preceded the loss of function of the A_1AR. Inhibition of NF-κB attenuated the increase in A_1AR induced by pertussis toxin. Cells exposed to B-oligomer subunit of pertussis toxin, devoid of significant ADP ribosyltransferase activity, showed increased A_1AR protein expression, preceded by activation of NF-κB. B-Oligomer increased intracellular Ca^{2+} in DDT_1 MF-2 cells. Chelation of intracellular Ca^{2+} with 1,2-bis(2-aminophenoxy)ethane-*N*,*N*,*N*′,*N*′-tetraacetic acid or inhibition of protein kinase C (PKC) with bisindolylmaleimide hydrochloride reduced the activation of NF-κB and [^{3}H]DPCPX binding. We conclude that pertussis toxin promotes de novo A_1AR synthesis by activating NF-κB through an ADP ribosylation-independent mechanism involving intracellular Ca^{2+} release and PKC activation.

Adenosine receptors (ARs) are members of the superfamily of heptahelical G protein-coupled receptors, which are the primary targets of endogenously released adenosine. To date, four types of ARs, namely A_1, A_{2a}, A_{2b}, and A_3AR, have been cloned and characterized from several mammalian species, including humans (Dunwiddie and Masino, 2001). The A_1AR interacts with pertussis toxin-sensitive G proteins, including G_i and G_o proteins. Activation of this receptor subtype leads to inhibition of adenylyl cyclase, although other effector targets such as the voltage-sensitive Ca^{2+} channels (Sperelakis, 1987), K^+ channels (Kurachi et al., 1986), and mitogen-activated protein kinase (Dickenson et al., 1998) have also been identified.

Similar to other G protein-coupled receptors, agonist exposure promotes desensitization of the A_1AR, a process associated with phosphorylation and down-regulation of the receptor (Stiles, 1991). In contrast, exposure to antagonist ligands is associated with increased expression and G protein coupling efficiency of the A_1AR (Stiles, 1991). These differential responses to agonists and antagonists might reflect the need of the cell to maintain homeostasis in the presence of excessive or chronic stimulation or inhibition of the receptor, re-

This work was supported in part by National Institutes of Health Grant HL-54279 and by funds from the Southern Illinois University School of Medicine.
Article, publication date, and citation information can be found at http://jpet.aspetjournals.org.
doi:10.1124/jpet.105.096255.

ABBREVIATIONS: AR, adenosine receptor; PKC, protein kinase C; NF-κB, nuclear factor κB; LPS, lipopolysaccharide; DPCPX, [^{3}H]cyclopentyl-1,3-dipropylxanthine; PDTC, pyrrolidine dithiocarbamate; BAPTA, 1,2-bis(2-aminophenoxy)ethane-*N*,*N*,*N*′,*N*′-tetraacetic acid; BIM, bisindolylmaleimide hydrochloride; PD098059, 2-[2-amino-3-methoxyphenyl]-4*H*-1-benzopyran-4-one; *R*-PIA, *R*-phenylisopropyladenosine; AB-MECA, 4-aminobenzyl-5′-*N*-methylcarboxamidoadenosine; ERK, extracellular signal-regulated kinase; DDT_1, ductus deferens tumor, CHAPS, 3-[(3-cholamidopropyl)dimethylammonio]-1-propanesulfonic acid; PBS, phosphate-buffered saline; PCR, polymerase chain reaction; bp, base pair(s); GAPDH, glyceraldehyde-3-phosphate dehydrogenase; DTT, dithiothreitol; PMSF, phenylmethylsulfonyl fluoride; AM, acetoxymethyl ester.

spectively. Furthermore, the receptor demonstrates differential binding affinities to agonist and antagonist ligands, depending on the degree of receptor-G protein coupling in adipocyte membrane preparations (Ramkumar and Stiles, 1988) and following reconstitution of purified preparations of the A_1AR and G_i proteins (Freissmuth et al., 1991).

Pertussis toxin, an exotoxin derived from *Bordetella pertussis*, has been widely employed as a research tool to study receptor signaling via G_i and G_o proteins and transducin (Murayama and Ui, 1983). This endotoxin is a heterohexameric protein that is structurally and functionally comprised of an A and a B subunit, common to many of the bacterial toxins (Kaslow and Burns, 1992). The A-protomer consists of a single peptide subunit (S1) that possesses ADP ribosyltransferase activity and catalyzes the transfer of ADP-ribose from NAD to the cysteine residue at the C terminus of the α-subunit of G_i and G_o proteins and transducin. The B-oligomer comprises the S2, S3, S4, and S5 subunits in a stoichiometry of 1:1:2:1 and is responsible for attachment to the surface of its target cells (Wong and Rosoff, 1996). One consequence of binding to the cell surface is ADP ribosylation and inactivation of G_i, G_o, and transducin, even though a number of other effects of the toxin have also been described previously (Wong and Rosoff, 1996).

We hypothesized that uncoupling of the A_1AR from G_i by pertussis toxin could mimic the effect of chronic A_1AR antagonist treatment, leading to alteration in receptor expression in a futile attempt to re-establish normal receptor function. Data presented in this manuscript confirm this hypothesis and indicate that, in addition to ADP ribosylation and uncoupling of the A_1AR, pertussis toxin mediates de novo synthesis of the A_1AR. This increase in A_1AR expression was mediated by an ADP ribosylation-independent but a Ca^{2+}/protein kinase C (PKC)-dependent activation of transcription factor, nuclear factor (NF)-κB.

Materials and Methods

Materials. Pertussis toxin, HEPES, Tris·HCl, soybean trypsin inhibitor, pepstatin, benzamidine, adenosine, bacterial lipopolysaccharide (LPS), adenosine deaminase, [^{3}H]cyclopentyl-1,3-dipropylxanthine (DPCPX), pyrrolidine dithiocarbamate (PDTC), 1,2-bis(2-aminophenoxy)ethane-*N*,*N*,*N*′,*N*′-tetraacetic acid (BAPTA), bisindolylmaleimide hydrochloride (BIM), and PD098059 were obtained from Sigma Chemical Co. (St. Louis, MO). *R*-Phenylisopropyladenosine (*R*-PIA) and 4-aminobenzyl-5′-*N*-methylcarboxamidoadenosine (AB-MECA) were from Boehringer-Mannheim Biochemicals (Indianapolis, IN). The antagonist radioligand [^{3}H]DPCPX (160 Ci/mmol), ^{125}I-sodium, and [^{32}P]α-dCTP (3000 Ci/mmol) were purchased from Du-Pont New England Nuclear (Boston, MA). Synthesis of ^{125}I-AB-MECA was performed as described previously (Olah et al., 1994). Antibodies against p65, p50, phosphor-extracellular signal-regulated kinase (ERK) 1/2, and total ERK1 were purchased from Santa Cruz Biotechnology (Santa Cruz, CA), whereas antibody against β-actin was from Sigma Chemical Co. Cell culture supplies, including Dulbecco's modified Eagle's medium (high-glucose) medium, fetal bovine serum, and penicillin-streptomycin were obtained from GIBCO-BRL (Grand Island, NY). All other reagents were of highest available grade and were purchased from standard sources.

Cell Culture. DDT_1 MF-2 cells were cultured in medium consisted of Dulbecco's modified Eagle's medium (high-glucose), supplemented with 10% fetal bovine serum, 50 U/ml penicillin, and 25 μg/ml streptomycin. Cells were grown at 37°C in the presence of 5% CO_2 and 95% ambient air. Cells were passaged twice a week, and all the experiments were performed using confluent monolayers.

Radioligand Binding Assay. Cells were detached in ice-cold phosphate-buffered saline containing 5 mM EDTA. The cells were then lysed in 10 mM Tris·HCl buffer (pH 7.4 at room temperature), containing 5 mM EDTA, 10 μg/ml soybean trypsin inhibitor, 10 μg/ml benzamidine, and 2 μg/ml pepstatin, and homogenized briefly by Polytron homogenizer (Brinkmann Instruments, Westbury, NY) at setting 8 for 20 s at 4°C. Membranes were obtained by centrifugation of the homogenates at 14,000*g* for 15 min. The final pellet was resuspended in 50 mM Tris·HCl buffer (pH 7.4 at room temperature), 10 mM $MgCl_2$, and 1 mM EDTA, containing protease inhibitors (described above). Endogenously released adenosine was degraded using adenosine deaminase (5 U/ml) and incubating the mixture for 15 min at 37°C. This preparation was then used for radioligand binding.

Quantitation of A_1AR was performed using the antagonist [^{3}H]DPCPX. Membrane preparations (approximately 80 μg of protein/assay tube) were incubated with the radioligands for 45 min at 37°C in the absence or presence of 1 mM theophylline (to define nonspecific binding) in a total volume 250 μl of 50 mM Tris·HCl, pH 7.4, 10 mM $MgCl_2$, and 1 mM EDTA. Saturation binding experiments were performed by incubating at least five concentrations of [^{3}H]DPCPX (0.5–5 nM) with membranes for 45 min at 37°C. The reaction mixture was then filtered over polyethylenimine-treated (0.3%) Whatman GF/B glass fiber filters (Whatman, Clifton, NJ) and washed with 10 ml of ice-cold Tris buffer containing 0.01% CHAPS. The radioactive content of each filter was determined using a Beckman liquid scintillation counter (LS5801; Beckman Instruments, Fullerton, CA) or a Packard (5780) gamma counter (PerkinElmer Life and Analytical Sciences, Boston, MA). Analyses of radioligand binding data were performed using GraphPad Prism (GraphPad Software, San Diego, CA).

Immunocytochemistry. DDT_1 MF-2 cells were cultured on cover slips, and respective treatments were done. Cells were then fixed with 4% paraformaldehyde for 15 min, washed twice with phosphate-buffered saline (PBS), and then exposed to PBS containing 5% normal donkey serum for 10 min to reduce nonspecific binding. Cells were treated with a mouse monoclonal A_1AR antibody diluted 1:5 in 5% normal donkey serum along with 0.05% Triton X-100 in PBS and incubated for 1 h at 37°C. Following incubation, cells were washed with PBS and treated for 1 h with donkey anti-mouse IgG labeled with rhodamine (Jackson Immunochemicals, West Grove, PA) diluted 1:100 in PBS, containing 5% normal donkey serum and 0.05% Triton X-100. Cells were then washed once with PBS and with 75% ethanol followed by a wash with water. The coverslips were then mounted on glass microscope slides using aqua-mount and visualized by a Fluoview confocal microscope (Olympus America Inc., Melville, NY) using a 20× objective.

RNA Preparation, Reverse Transcription, and Polymerase Chain Reaction. Isolation of total RNA from DDT_1-MF2 cells was performed by using Tri reagent (Sigma), as directed by the manufacturer. Total RNA was then used to prepare the poly(A)$^+$RNA, which was reverse transcribed using an iScript cDNA synthesis kit (Bio-Rad, Hercules, CA) in a total volume of 20 μl. Two microliters of the reaction volume was then used for polymerase chain reaction (PCR) amplification. PCR reactions were performed in a total volume of 25 μl. Primer sequences for A_1AR included 5′-CAT CCC ACT GGC CAT CCT TAT-3′ (sense) and 5′-AGG TAT CGA TCC ACA GCA ATG-3′ (antisense), which predictably generated a 115-bp PCR product. PCR conditions used were 94°C for 5 min for denaturation, 45 cycles of 94°C for 30 s, 64°C for 15 s, and 72°C for 30 s in that order and finally an extension time of 10 min at 72°C. The respective products were normalized to glyceraldehyde-3-phosphate dehydrogenase (GAPDH). The primer sequences included 5′-ATG GTG AAG GTC GGT GTG AAC-3′ (sense) and 5′-TGT AGT TGA GGT CAA TGA AGG-3′ (antisense), and the PCR product was seen at 110 bp. All the PCR products were resolved on a 2.0% agarose gel containing SYBR Green I (Life Technologies Inc., Carlsbad, CA). Bands of interest were visual-

ized and quantitated using the Un-Scan-It software (Silk Scientific Inc., Orem, UT).

Real-Time PCR. Total RNA was isolated, and poly(A)$^+$RNA was made from it as described above. Poly(A)$^+$RNA (1 μg) was converted to c-DNA using iScript cDNA Synthesis Kit (Bio-Rad). The reaction mixture was set up as follows: 15 μl of poly(A)$^+$RNA, 4 μl of iScript reaction mix, and 1 μl of iScript reverse transcriptase in the total volume of 20 μl. The reaction mix was incubated at 25°C for 5 min, 42°C for 30 min, and 85°C for 5 min. The cDNA reaction mix was then used for real-time PCR. The primers used for A_1AR were identical to those used for traditional PCR (above). The reaction mixture for real-time PCR was set up as follows: 2 μl of c-DNA, 0.5 μl of each primer (50 pM stock), and 12.5 μl of the iQ SYBR Green Supermix reagent (Bio-Rad) in a total volume of 25 μl of DNase/RNase-free water. GAPDH was used for normalization and set up as follows: 1 μl of cDNA, 12.5 μl of the iQ SYBR Green Supermix reagent, and 1 μl of GAPDH primer in a final volume of 25 μl of DNase/RNase. The primers used for GAPDH were identical to those described above for traditional PCR. Amplification and detection was performed with the Cepheid Smart Cycler Detection System (Cepheid, Sunnyvale, CA). Negative control reactions for A_1AR and GAPDH were set up as above without any template cDNA. Cycling conditions were 95°C for 3 min followed by 65 cycles at 95°C for 15 s, 64°C for 30 s, and 72°C for 30 s. On completion of amplification, melting curve analysis was performed by cooling the reaction to 60°C and then heating slowly until 95°C according to the instructions of the manufacturer (Cepheid). The cycle number at which the sample reaches the threshold fluorescent intensity is called the cycle threshold (Ct). The relative change in mRNA levels between control (a) and pertussis-toxin treated sample (b) was measured using the formula $2^{(\text{Ct Target gene a} - \text{Ct GAPDH1}) - (\text{Ct Target gene b} - \text{Ct GAPDH2})}$. Relative changes in A_1AR RNA levels between samples have been expressed as percentage of normal control. Negative controls for both the A_1AR gene and GAPDH were used for all reaction groups. Real-time PCR products were also run on a 2.0% agarose gel, and the 115-bp product size was verified.

Western Blotting. Total cell lysates were used to quantitate *R*-PIA-mediated activation of ERK1/2, whereas nuclear extracts were used for NF-κB subunits. Nuclear extracts were prepared in 10 mM HEPES, pH 7.9, 10 mM KCl, 0.1 mM EDTA, 0.4% Nonidet P-40, 1 mM dithiothreitol (DTT), and 1 mM phenylmethylsulfonyl fluoride (PMSF) (buffer A). The mixtures were centrifuged at 5000*g* for 30 s, and the cytosolic extract was separated. The nuclear pellet was washed with excess volume of buffer A and then resuspended in 20 mM HEPES, pH 7.9, 400 mM NaCl, 1 mM EDTA, 1 mM DTT, and 1 mM PMSF (buffer B). After incubating for 5 min at 4°C with rotation, the extracts were centrifuged (5000*g*, 1 min), and the supernatants were used for Western blotting. Proteins were transferred to nitrocellulose membranes, blocked in a solution containing 130 mM NaCl, 2.7 mM KCl, 1.8 mM Na_2HPO_4, 1.5 mM KH_2PO_4, 0.1% NaN_3, 0.1% Triton X-100, and 5% low-fat skim milk for 1 h, and then incubated at 4°C overnight with primary antibody. After five washes in blocking solution, blots were incubated with horseradish peroxidase-labeled goat anti-rabbit IgG or rabbit anti-goat IgG secondary antibody (Santa Cruz Biotechnology) for 1 h at room temperature and washed three times with Tris-buffered saline (20 mM Tris·HCl and 137 mM NaCl, pH 7.6, at 25°C), containing 0.1% Tween 20. This was followed by three washes with Tris-buffered saline without Tween 20, treatment with ECL Plus reagents (Amersham Biosciences, Piscataway, NJ), and visualization by exposure to Kodak XAR film (Fisher Scientific, Pittsburgh, PA) or by using a charge-coupled device camera (Hitachi Genetic Systems, MiraiBio Inc., Alameda, CA). Bands were quantified using the Un-Scan-It software.

Electrophoretic Mobility Shift Assay. Electrophoretic mobility shift assay was performed by incubating nuclear extracts with ^{32}P-radiolabeled double-stranded oligonucleotide probes suspended in reaction buffer (12 mM HEPES, pH 7.9, 100 mM NaCl, 0.25 mM EDTA, 1 mM DTT, and 1 mM PMSF) at room temperature for 10 min. The protein-DNA complexes were electrophoresed using 4% nondenaturing polyacrylamide gels, dried, and exposed to X-ray films (Fisher Scientific) or to phosphor screen imaging (Cyclone Storage Phosphor System, PerkinElmer Life and Analytical Sciences). The -fold increase in the expression of the transcription factors was determined using background subtract. The oligonucleotide probes used in these assays were 5′-CAACGGCAGGGGAATTCCCCTCTCCTT-3′ (for NF-κB) and 5-TGTCGAATGCAAATCACTAGAA-3′ (for Oct-1).

Ca^{2+} Imaging. To detect changes in intracellular Ca^{2+} levels, DDT_1 MF-2 cells were cultured on glass coverslips. Adherent cells were washed with physiologic buffer (130 mM NaCl, 4 mM KCl, 10 mM HEPES, 5 mM glucose, 2 mM $CaCl_2$, and 2 mM $MgCl_2$, pH 7.3) and loaded with 5 μM Fluo-4, AM (Molecular Probes, Eugene, OR). After incubation at 37°C for 30 to 45 min, the cells were washed once with physiologic buffer and imaged with an Argon laser at 488 nm using flow view confocal microscope. Baseline images were recorded in the presence of vehicle and for 15 min following addition of B-oligomer. Analysis of the image obtained was carried out using the Fluoview software.

Protein Determination. The levels of protein in samples were determined by the method of Bradford (1976), using bovine serum albumin to prepare standard curves.

Statistical Analysis. Statistical analyses were performed using analysis of variance and Dunnett's post hoc test. Error bars shown in the figures represent S.E.M.

Results

Pertussis Toxin Uncouples the A_1AR from Its G Protein(s). Treatment of DDT_1 MF-2 cells with pertussis toxin (100 ng/ml) produced a time-dependent decrease in the binding of the A_1AR agonist radioligand ^{125}I-AB-MECA, which was reduced by 67 ± 3% at 8 h and 76 ± 5% by 12 h (Fig. 1A). Because the agonist radioligand interacts with high affinity to A_1AR coupled to the G_i proteins expressed in the plasma membranes of these cells, a decrease in binding reflects uncoupling of the A_1AR from G_i proteins by pertussis toxin. In contrast, the binding of the antagonist radioligand, [^{3}H]DPCPX, showed a time-dependent increase by ~4 h and progressive elevations up to 12 h (Fig. 1B). The binding of the antagonist radioligand was increased by 117.3 ± 34.1% after 8 h and 149.4 ± 24.7% following 12 h of exposure to pertussis toxin, with no further significant change by 24 h.

To determine whether pertussis toxin functionally uncouples the A_1AR from its G proteins, we determined whether it inhibits A_1AR-stimulated phosphorylation of ERK1/2. The addition of 1 μM *R*-PIA to cultures increased ERK1/2 phosphorylation, which peaked at 5 min and returned to basal level by 30 min. The phosphorylation of ERK1/2 was abrogated in cells pretreated with pertussis toxin (100 ng/ml) for 12 h, a time point at which significant uncoupling of the A_1AR was observed (Fig. 1C). Similarly, cells pretreated for 30 min with 20 μM PD098059, an inhibitor of mitogen-activated protein kinase kinase, showed reduced stimulation of ERK1/2 phosphorylation. These findings suggest that optimal inactivation of G_i had occurred during the 12-h treatment of cells with pertussis toxin and that A_1AR-stimulated ERK1/2 phosphorylation is mediated via a G_i pathway.

We also observed inhibition of basal (time 0) ERK1/2 phosphorylation by pertussis toxin. Pretreating cells with DPCPX (1 μM) or adenosine deaminase (5 U/ml) reduced basal ERK1/2 phosphorylation (Fig. 1D), implicating endogenous

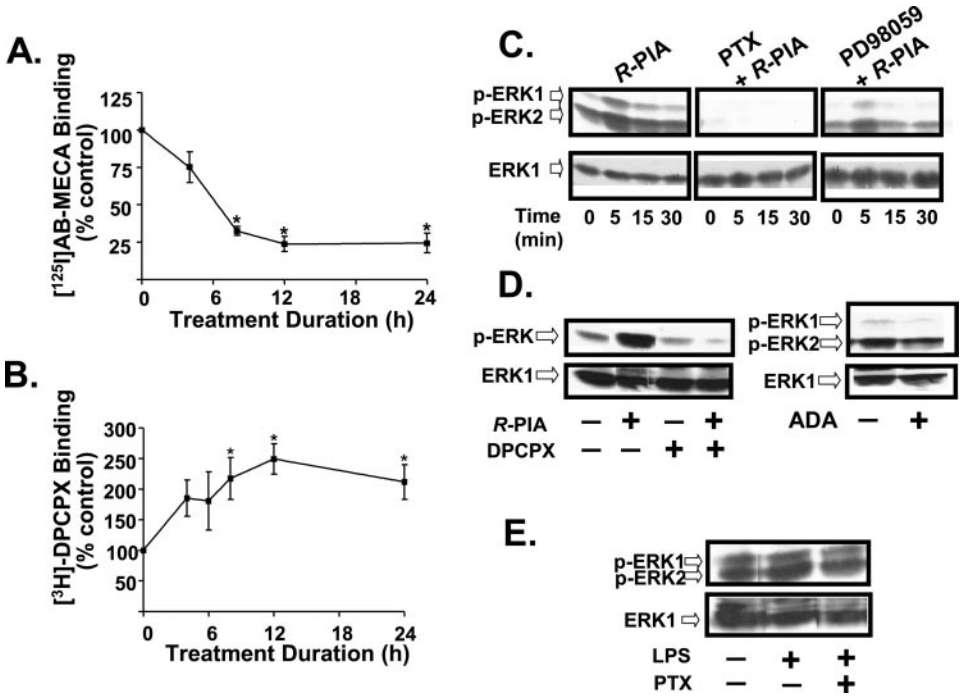

Fig. 1. Pertussis toxin uncouples the A_1AR from its associated G proteins. A and B, DDT_1 MF-2 cells were treated with pertussis toxin (100 ng/ml), and the binding of the agonist (^{125}I-AB-MECA) (A) and the antagonist ([^{3}H]DPCPX) radioligands (B) were assessed in crude membrane preparations at different times over 24 h. Data are presented as the mean ± S.E.M. of four independent experiments. Asterisks indicate statistical significant difference from control ($p < 0.05$). C, pertussis toxin abolishes *R*-PIA-dependent ERK1/2 phosphorylation. Cells were exposed to pertussis toxin (100 ng/ml) for 12 h or to PD98059 (20 μM) for 30 min prior to the addition of *R*-PIA (1 μM) for the time periods indicated. Cells were washed with phosphate-buffered saline containing phosphatase inhibitors, and lysates were prepared and resolved by 12% SDS-polyacrylamide gel electrophoresis. Gels were blotted on to nitrocellulose membranes and visualized by using phosphoERK1/2 or total ERK1 polyclonal primary antibodies and an horseradish peroxidase-tagged secondary antibody. D, basal ERK1/2 phosphorylation is inhibited by treating the cells with either 1 μM DPCPX or 5 U/ml adenosine deaminase (ADA), implicating the role of endogenous adenosine acting at the A_1AR. E, pertussis toxin did not inhibit LPS-stimulated ERK1/2 phosphorylation. DDT_1 MF-2 cells were pretreated with pertussis toxin (100 ng/ml) for 12 h, followed by 15-min treatment with 3 μg/ml LPS.

adenosine in the activation of this kinase under basal condition. However, pertussis toxin treatment did not significantly reduce the stimulation of ERK1/2 by LPS (Fig. 1E), which occurs independent of G_i, discounting a nonspecific inhibitory effect of pertussis toxin on ERK1/2.

Pertussis Toxin Increases the Affinity and Expression of the A_1AR. A previous study indicated that uncoupling of the A_1AR from the G_i protein by guanine nucleotides altered the affinity of the receptor for ligands (Ramkumar and Stiles, 1988). To determine whether the increase in [^{3}H]DPCPX binding, observed above, reflects an increase in affinity of this receptor and/or results from an increase in number of the A_1AR, full saturation plots were performed on membranes obtained from control and pertussis toxin-treated cells (Fig. 2A). Analysis of these curves indicate a statistically significant increase in the B_{max} from 206 ± 24 to 321 ± 26 fmol/mg protein ($p < 0.05$) in the cells treated with pertussis toxin (100 ng/ml) for 12 h (inset). Interestingly, saturation plots obtained from membranes of pertussis toxin-treated cells showed consistently higher affinities for the radioligand, as depicted by a reduction in the equilibrium dissociation constant (K_d) values. K_d values were 0.75 ± 0.07 nM for controls and 0.34 ± 0.08 nM for pertussis toxin-treated cells (inset). To determine whether the increase in B_{max} reflected a true increase in the number of the A_1AR, immunocytochemistry was performed using a monoclonal antibody for A_1AR (Ochiishi et al., 1999) and rhodamine-conjugated secondary antibody. Detection of the labeled A_1AR was determined by confocal microscopy, which showed the receptor as a reddish-orange color localized primarily to the cell surface, but with some cytosolic staining (Fig. 2B). Qualitatively, there was a substantial increase in A_1AR fluorescence observed in the cells treated with pertussis toxin, confirming that the increase in B_{max} was most likely due to an increase in the A_1AR protein. All of the treatment groups were processed simultaneously with the antibody and visualized using the same settings on the confocal microscope, ensuring appropriate comparisons of the treatment groups. No immunolabeling was observed in the absence of primary antibody addition, indicating antibody specificity.

Pertussis Toxin Increases Transcription of the A_1AR Gene. We next determined the expression of A_1AR transcripts in control cells and the cells treated with pertussis toxin. DDT_1 MF-2 cells treated with pertussis toxin for 8 h showed an increase in A_1AR mRNA, as depicted qualitatively by reverse transcription-PCR (Fig. 3A). The quantitative evaluation of mRNA synthesis by real-time PCR demonstrated 7.3 ± 0.8-fold increase in the A_1AR mRNA content (normalized to GAPDH mRNA) in pertussis toxin-treated cells, compared with the control cells (Fig. 3B).

Increase in A_1AR by Pertussis Toxin Involves NF-κB Activation. A previous study (Nie et al., 1998) has shown that upstream regulatory sites of the A_1AR gene contain consensus sequences for NF-κB, which mediates oxidative stress-induced A_1AR expression. To determine whether NF-κB mediates a similar induction of A_1AR mRNA by pertussis toxin, electrophoretic mobility shift assays were performed. Treatment of DDT_1 MF-2 cells with pertussis toxin

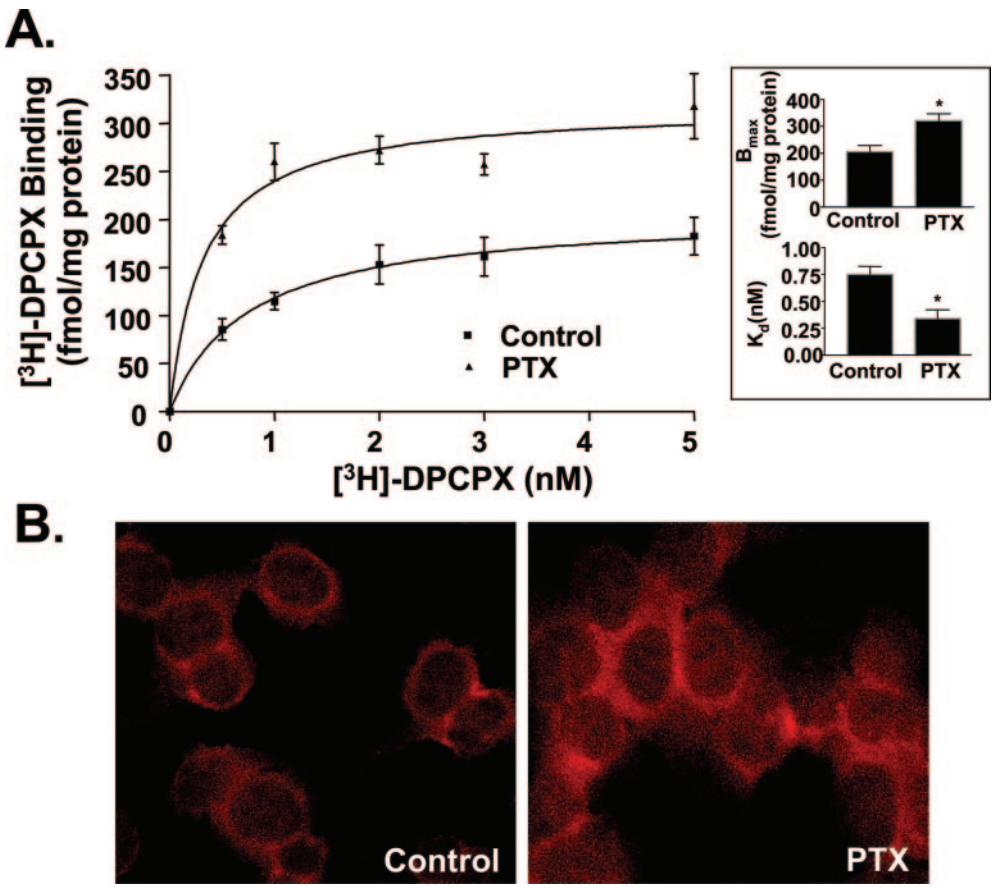

Fig. 2. Pertussis toxin treatment increases the number and affinity of the A_1AR. A, DDT_1 MF-2 cells were treated with pertussis toxin (100 ng/ml) for 12 h and used for [^{3}H]DPCPX radioligand binding assays. Inset (right) shows the significant change in B_{max} and K_d for A_1AR antagonist in the presence of pertussis toxin, as calculated from Scatchard analysis (GraphPad Prism Software). Values are expressed as the mean ± S.E.M. from four independent experiments. Asterisk indicates statistically significant difference ($p < 0.05$) from control (untreated) cells. B, immunocytochemistry was performed on cells treated for 12 h with pertussis toxin (100 ng/ml) using a mouse monoclonal antibody for the A_1AR and a rhodamine-tagged secondary antibody. Labeled cells were visualized by confocal microscopy using 200-fold magnification.

led to a rapid increase in NF-κB activity, observed as early as 30 min following exposure to the toxin (Fig. 4A). To identify the subunit(s) of NF-κB activated in this process, supershift assays were carried out using the specific antibodies against most commonly expressed p65 and p50 subunits of this complex. Figure 4A demonstrates the presence of supershifted bands for p65, and p50, suggesting the involvement of both of these subunits in the activation of NF-κB by pertussis toxin. Normalization of all the blots was performed with a labeled oligonucleotide probe for Oct-1. This finding was further supported by Western blotting experiments for the p65 and p50 subunits using the same nuclear extracts used for electrophoretic shift mobility assays. Figure 4B is a representative Western blot showing increases in p50 and p65 present in the nucleus following exposure of cells to pertussis toxin for 30 min. To determine whether the increase in NF-κB activity was associated with the increase in A_1AR expression, cells were pretreated with PDTC (50 μM), an inhibitor of NF-κB, 1 h prior to the administration of pertussis toxin, and [^{3}H]DPCPX binding was performed on the membranes prepared from these cells (Fig. 4C). We observed a significant reduction ($p < 0.05$) in the response to pertussis toxin by PDTC. The decreased expression of A_1AR by PDTC was confirmed by A_1AR immunoreactivity (Fig. 4D).

Activation of NF-κB by Pertussis Toxin Is Independent of ADP Ribosylation Activity. The rapid rate of activation of NF-κB by pertussis toxin (~30 min) suggests that this process likely does not involve ADP ribosylation of G_i, which occurs several hours after exposure to pertussis toxin (see Fig. 1). Recent data have implicated B-oligomer moiety of the holotoxin, devoid of ADP ribosyltransferase activity, in regulating the activity of NF-κB (Iordanskiy et al., 2002; Tonon et al., 2002). Therefore, we next determined whether B-oligomer activates NF-κB in DDT_1MF-2 cells. Cells were incubated with various concentrations of B-oligomer for 30 min, and samples were prepared for electrophoretic mobility shift assays. As shown in Fig. 5A, B-oligomer increased the activity of NF-κB in a dose-dependent manner, with maximal effects observed at 30 min using 100 nM of the subunit. As would be expected for NF-κB activation, B-oligomer administration stimulated the degradation of the inhibitory IκB-α protein. Maximum decrease in IκB-α was obtained after 20 min of B-oligomer treatment and partially recovered by 30 min, possibly indicative of de novo protein synthesis (Sun et al., 1993). To test whether activation of NF-κB by B-oligomer correlates with the induction of A_1AR, we performed [^{3}H]DPCPX binding. As shown in Fig. 5C, treatment with B-oligomer (1 nM) produced a 121% increase in A_1AR at 12 h. There was no significant loss of agonist radioligand binding using the same treatment conditions (Fig. 5D), confirming that this preparation of B-oligomer was devoid of significant ADP ribosyltransferase activity. This was further supported by experiments that showed that cells incubated with B-oligomer for 6 h, a time point associated with a significant increase in [^{3}H]DPCPX binding, demonstrate no significant reduction in *R*-PIA-stimulated ERK1/2 phosphorylation (Fig. 5D, inset). Similar to the increased [^{3}H]DPCPX binding, we also observed increases in A_1AR immunoreactivity in cells treated with B-oligomer, which was reduced by PDTC (Fig. 5E).

Activation of NF-κB by B-Oligomer Involves an Increase in Intracellular Ca^{2+} Release. A previous study

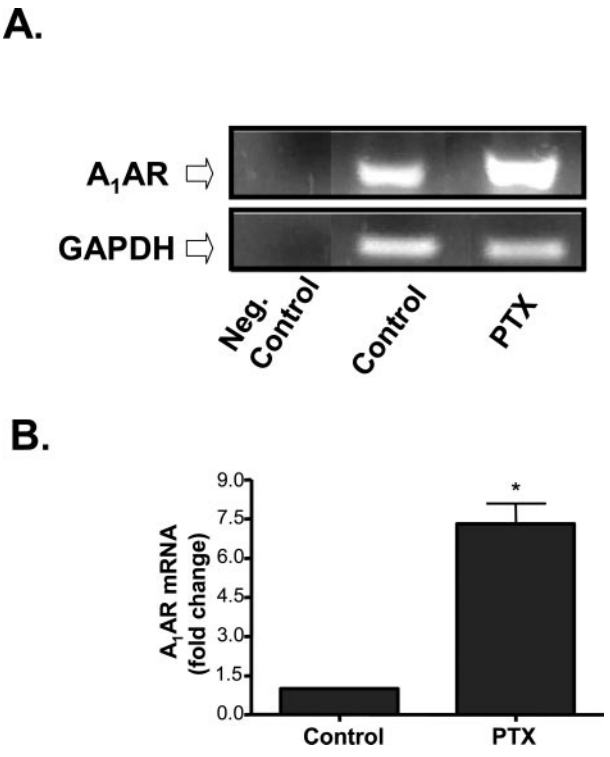

Fig. 3. Pertussis toxin increases A_1AR transcripts. A, reverse transcription-PCR and quantitative real-time PCR studies were performed using selective primers for the A_1AR and poly(A)$^+$ RNA, as detailed under *Materials and Methods*. The figure is a representative electrophoresis gel picture showing the increased A_1AR mRNA expression in the presence of pertussis toxin obtained after 36 cycles. GAPDH was used for normalization. B, quantitative analysis of A_1AR mRNA expression by real-time PCR. The data represent the mean ± S.E.M. of three independent experiments. Asterisk indicates statistically significant difference ($p < 0.05$) from control.

demonstrated a critical role of intracellular Ca^{2+} in mediating activation of NF-κB by oxidant stress in the endoplasmic reticulum (Pahl and Baeuerle, 1996). To determine the pathway(s) involved in the activation of NF-κB by B-oligomer, we determined whether this agent increases intracellular Ca^{2+} release. We observed an increase in intracellular Ca^{2+} release in DDT_1MF-2 cells following a 15-min exposure to B-oligomer (Fig. 6A). To determine whether this increase in intracellular Ca^{2+} was involved in the activation of NF-κB, Ca^{2+} was chelated by adding BAPTA-AM (20 μM) 30 min prior to B-oligomer treatment. BAPTA-AM significantly reduced B-oligomer-dependent NF-κB activation by ~50% (Fig. 6B). In addition, BAPTA-AM reduced B-oligomer-induced increase in [^{3}H]DPCPX binding, indicative of an increase in A_1AR. B-oligomer increased [^{3}H]DPCPX binding from 416 ± 72 to 793 ± 20 fmol/mg protein, which was reduced to 441 ± 30 fmol/mg protein in cells pretreated with BAPTA-AM. The addition of BAPTA-AM alone produced a small but insignificant reduction in [^{3}H]DPCPX binding.

One of the downstream signaling molecules activated by rise in intracellular Ca^{2+} is PKC. Therefore, we next determined whether PKC plays a role in the activation of NF-κB by B-oligomer by electrophoretic mobility shift assays. Inhibition of protein kinase C with 1 μM BIM reduced the B-oligomer activation of NF-κB by more than 50%. Quantitation of A_1AR by radioligand binding assays indicated a decrease in receptor by BIM in B-oligomer-treated cells. B-Oligomer increased [^{3}H]DPCPX binding by 76 ± 13% over control and by 36 ± 4% in the presence of BIM (Fig. 7B).

Discussion

Inhibition of receptor function in biological systems is generally countered by an increased expression and function of the receptor and/or postreceptor signaling proteins that serve as the targets for inhibition. This homeostatic mechanism allows for the receptor system to maintain some level of activation or recharges it for activity once the inhibitor is removed. In this study, we determined the consequences of functional inactivation of the A_1AR by ADP ribosylation of its coupling G_i protein by pertussis toxin. Our data indicate that pertussis toxin stimulates A_1AR expression by activating NF-κB in these cells. Interestingly, this response seems to be independent of ADP ribosylation of G_i because it is also observed with the B-oligomer subunit of the toxin that is devoid of significant ADP ribosyltransferase activity. However, B-oligomer-mediated increase in intracellular Ca^{2+} release and possibly activation of PKC could account for the activation of NF-κB and induction in A_1AR.

The A_1AR has been extensively studied to determine the mechanism(s) underlying agonist-induced receptor desensitization. Agonist exposure resulted in reduced A_1AR-mediated functions in cultured rat adipocytes (Green, 1987), in cardiac myocytes (Shryock et al., 1989), in DDT_1 MF-2 cells (Ramkumar et al., 1991), and in the cells transfected with the A_1AR cDNA (Palmer and Stiles, 1995). Similarly, in vivo studies have documented agonist-induced desensitization of the A_1AR in the rat adipocytes (Longabaugh et al., 1989) and rat brain (Ruiz et al., 1996). The aforementioned in vivo study indicates that desensitization of the A_1AR affects multiple components of the A_1AR signaling pathway, which include both the receptor and the associated G_i proteins. In contrast, administration of the antagonist caffeine to rats increased A_1AR levels along with its G proteins (Ramkumar et al., 1988).

In this study, we demonstrated that pertussis toxin treatment uncouples the A_1AR from the G_i coupling protein, as indicated by a loss of high-affinity agonist binding and a decrease in A_1AR-mediated phosphorylation of ERK1/2. This was associated with a time-dependent increase in antagonist binding. The time points at which increases in antagonist binding were observed were similar to the time course of receptor uncoupling, suggesting that both events were occurring simultaneously. We have shown previously a similar alteration in the binding of the xanthine amino congener antagonist radioligand in adipocyte membrane preparations when receptor uncoupling was initiated by guanine nucleotides (Ramkumar and Stiles, 1988). We proposed that the native A_1AR conformation allows for tight coupling to its G proteins and high-affinity agonist binding, which is altered by uncoupling. On the other hand, the antagonist interacts preferentially with the uncoupled A_1AR. Together, these data suggest that the agonist and antagonist ligands are interacting with different conformations of the A_1AR, as suggested by Barrington et al. (1989). Using chimeric A_1/A_3AR, Olah et al. (1994) indicate that different segments of the A_1AR confer high-affinity agonist and antagonist binding. They show that transmembrane regions 4, and to a lesser extent, transmembrane regions 6 and 7, are involved in the

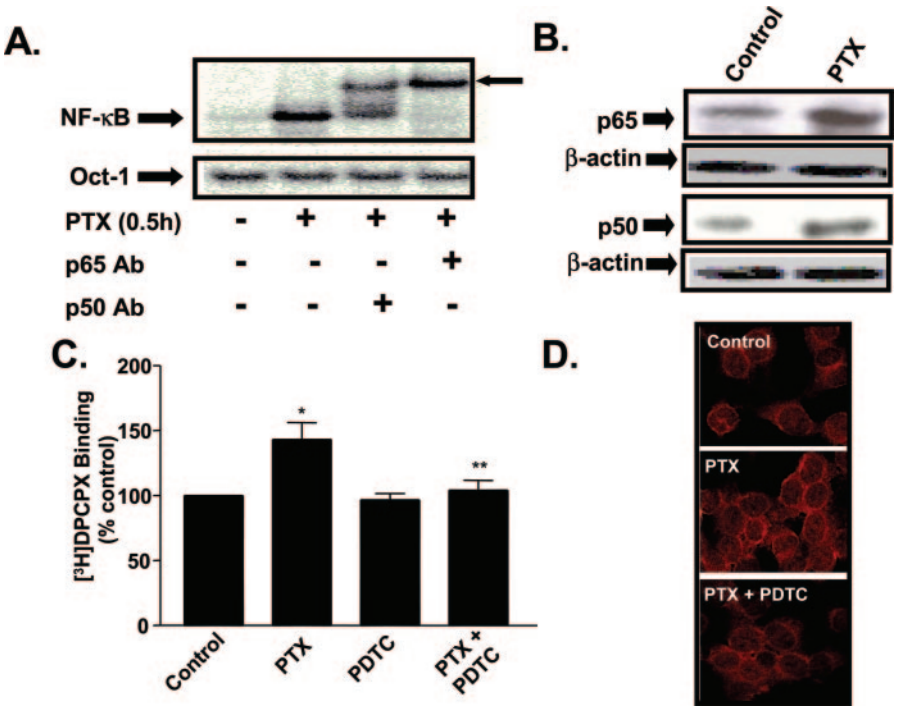

Fig. 4. Activation of NF-κB by pertussis toxin mediates the induction in A_1AR expression. A, cells were treated with pertussis toxin (100 ng/ml) for 0.5 h, and nuclear extracts were prepared and were used for assessing NF-κB activity by electrophoretic mobility shift assays. For supershift assays, nuclear preparations were incubated with 2 μg of p50 or 2 μg of p65 polyclonal antibody prior to performing electrophoretic mobility shift assays, and the supershifted bands are identified as bands with apparent higher molecular weights (see arrow). A labeled Oct-1 primer was used for normalization of the data. B, levels of p50 and p65 subunits in the nucleus following a 30-min exposure of cells to pertussis toxin was identified by Western blotting and normalized by β-actin. C, increase in A_1AR by pertussis toxin was inhibited by pretreating cells with 50 μM PDTC, an inhibitor of NF-κB. Cells were exposed to their respective treatment groups for 12 h, and plasma membrane fractions were used for antagonist [^{3}H]DPCPX radioligand binding. *, $p < 0.05$, statistical significant difference from control. **, $p < 0.05$, statistical significant difference from cells treated with pertussis toxin alone. D, A_1AR immunolabeling was performed on the cells following indicated treatments, and fluorescence was visualized using a confocal microscope at 200-fold magnification. Image is a representative of a set of at least three independent experiments performed under similar conditions.

binding of the A_1AR antagonist (Olah et al., 1994). Another possible explanation for the increased antagonist affinity is that the A_1AR is bound to the endogenous agonist, adenosine, under normal condition and that this is disrupted by pertussis toxin. As such, the antagonist would have unimpeded access to the receptor following pertussis toxin treatment. To reduce this possibility, we routinely pretreated membranes with adenosine deaminase at a concentration of 5 U/ml to degrade the endogenously released adenosine.

A second property of pertussis toxin was its ability to induce A_1AR by activating NF-κB. This transcription factor exists in cytoplasm as homodimeric or heterodimeric proteins, where it is sequestered by IκB proteins. Activation of NF-κB results from phosphorylation of IκB-α at serine 32 and 36, followed by polyubiquitination and degradation via 26 S proteosomal pathway. The degradation of IκB-α unmasks a nuclear localization sequence present on the NF-κB protein dimers, thereby promoting nuclear translocation and DNA binding activity (Ghosh et al., 1998).

We have shown previously that oxidative stress promotes nuclear translocation and binding of NF-κB to an upstream consensus sequence and promotes A_1AR gene activity (Nie et al., 1998). We observed increases in NF-κB activity as early as 30 min following exposure of DDT_1 MF-2 cells to pertussis toxin, a time point not associated with ADP ribosylation of G_i. Exposure to B-oligomer, which produced no significant uncoupling of the A_1AR from G_i at the concentrations used, also activated NF-κB and increased A_1AR. Thus, activation of NF-κB and increase in A_1AR by pertussis toxin is independent of ADP ribosylation of G proteins.

Unlike our findings, Ishibashi and Nishikawa (2003) reported activation of NF-κB in human bronchial epithelial cells following *B. pertussis* infection, but an abrogation of NF-κB activity following exposure to the purified pertussis toxin. Furthermore, Iordanskiy et al. (2002) showed inhibition of NF-κB by B-oligomer subunit of pertussis toxin in U-937 promonocytic cells. However, our results corroborate those of Tonon et al. (2002), who showed activation of NF-κB in monocyte-derived dendritic cells by a mutant form of pertussis toxin devoid of ADP-ribosylating activity.

Several pieces of evidence support a role of Ca^{2+} in the activation of NF-κB. In neurons, for example, intracellular Ca^{2+} maintains the basal activity of NF-κB (Lilienbaum and Israel, 2003), whereas a rise in intracellular Ca^{2+} by glutamate promotes NF-κB activation (Mattson and Camandola, 2001). Similarly, oxidant stress in the endoplasmic reticulum stimulates NF-κB by increasing Ca^{2+} levels within the cell (Pahl and Baeuerle, 1996). Oxidant challenge in Jurkat T cells and Wurzburg cells activated NF-κB via an increase in intracellular Ca^{2+} release (Sen et al., 1996). Our findings suggest a similar role of intracellular Ca^{2+} in the activation of NF-κB by pertussis toxin and B-oligomer in DDT_1 MF-2 cells. A similar rise in intracellular Ca^{2+} levels was demonstrated by pertussis toxin/B-oligomer in platelets and T lymphocytes and results from interaction with specific receptors

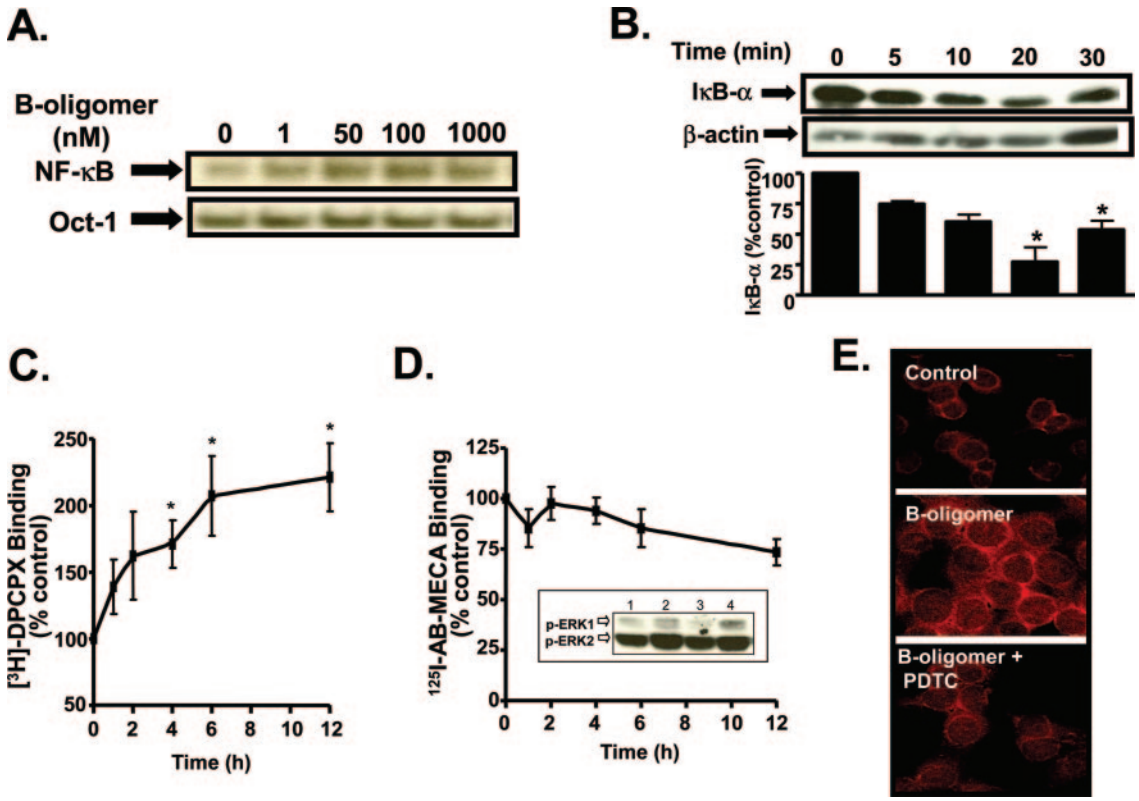

Fig. 5. B-Oligomer increases NF-κB-dependent A_1AR expression independent of receptor-G_i uncoupling. A, DDT_1 MF-2 cells were exposed to different concentrations of B-oligomer for 0.5 h. Nuclear fractions were obtained, and electrophoretic mobility shift assays were performed as described under *Materials and Methods* and normalized to Oct-1 DNA binding activity. The data indicate a dose-dependent increase in NF-κB activation, starting with 1 nM B-oligomer. B, B-oligomer-mediated NF-κB activation was also determined by assessing the degradation of IκB-α. Cells were treated with 1 nM B-oligomer for indicated time points, and whole-cell lysates were used for Western blotting to determine the levels of IκB-α protein. The data indicate maximal decrease in IκB-α levels by 20 min with partial recovery by 30 min. Bar graphs show the levels of IκB-α normalized to β-actin levels. C and D, plasma membranes obtained from control cells and those treated with B-oligomer (1 nM) for different time periods were used in [^{3}H]DPCPX and ^{125}I-AB-MECA binding assays. The data represent the mean ± S.E.M. of at least three independent experiments. Although [^{3}H]DPCPX binding showed a time-dependent increase, no significant change in the agonist radioligand binding was observed over the 12-h treatment with B-oligomer, indicating no receptor uncoupling during this period. Inset, treatment of cells with B-oligomer for 6 h did not affect the *R*-PIA-stimulated ERK1/2 phosphorylation. Labels 1 to 4 represent control, *R*-PIA (1 μM), B-oligomer (1 nM), and B-oligomer + *R*-PIA, respectively. E, immunocytochemistry for the A_1AR was performed on cells that were untreated, treated with B-oligomer for 12 h, or pretreated with PDTC for 30 min, followed by B-oligomer for 12 h. Rhodamine-labeled A_1ARs were visualized by confocal microscopy at 200-fold magnification.

such as glycoprotein 1b (Sindt et al., 1994) and CD3 (Gray et al., 1989), respectively.

One of the downstream signaling molecules involved in the Ca^{2+}-mediated activation of NF-κB is PKC. Pertussis toxin activates phospholipase C in platelets (Banga et al., 1987) and could therefore conceivably activate PKC in DDT_1 MF-2 cells. PKC phosphorylates and activates IκB kinase complex and thereby promotes the phosphorylation and degradation of IκB-α (Moscat et al., 2002), a prerequisite for translocation of NF-κB homo- and heterodimers to the nucleus. PKC has also been shown to be involved in LPS-induced NF-κB activation in neutrophils (Asehnoune et al., 2005). B cells isolated from the PKC-β-deficient mice show a defect in the IκB kinase complex phosphorylation and decreased NF-κB activation (Saijo et al., 2002).

Another mechanism by which a rise in intracellular Ca^{2+} couples to activation of NF-κB involves activation of calcineurin. This is suggested from studies in dendritic cells that show that LPS-stimulated NF-κB activation is mediated through a Ca^{2+}- and a cyclosporine A-sensitive pathway (Lyakh et al., 2000). Our data indicate attenuation of B-oligomer activation of NF-κB by inhibiting PKC, supporting a role of this kinase in this process. However, inhibition of calcineurin by cyclosporine A failed to have any effect on the B-oligomer-mediated NF-κB activation (data not shown). The lack of complete inhibition of NF-κB or induction in A_1AR by BAPTA or BIM may indicate incomplete inhibition of intracellular Ca^{2+} release or PKC activity, respectively, by the concentrations of these agents used in this study. Another possibility is that other pathway(s), in addition to these two outlined, promote the activation of NF-κB. A third possibility is that increases in intracellular Ca^{2+} release and PKC activation are occurring simultaneously and not sequentially, as would be expected if the increase in intracellular Ca^{2+} promotes activation of PKC.

Adenosine has been implicated in various lung pathologies, including asthma and chronic obstructive pulmonary disease. The levels of adenosine are elevated in bronchial lavage samples obtained from asthmatics. Furthermore, inhalation of adenosine promotes bronchoconstriction in the asthmatics but not in nonasthmatics. One of the targets of adenosine includes the A_1AR on bronchiolar smooth muscle (Abebe and Mustafa, 1998). *B. pertussis* adheres to the epithelial cell lines derived from the human respiratory tract. Infection with this organism is associated with bronchopneumonia and increased airway mucus secretion. The elaboration of B-oli-

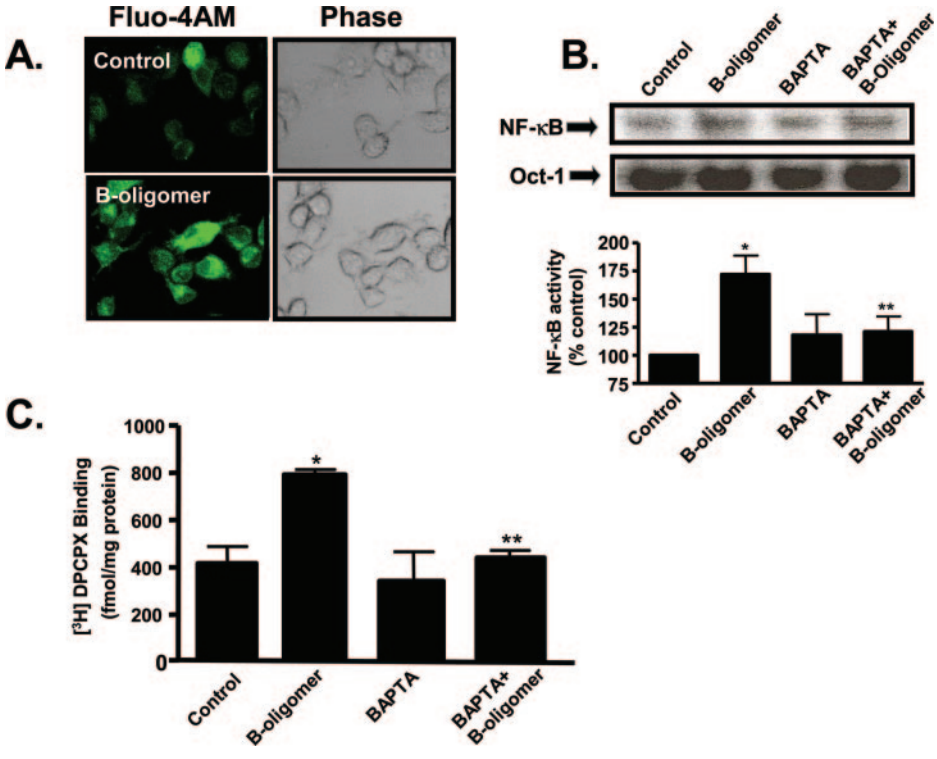

Fig. 6. B-Oligomer activates NF-κB by increasing intracellular Ca^{2+} release. A, DDT_1 MF-2 cells were exposed to vehicle or 1 nM B-oligomer for 15 min, and intracellular Ca^{2+} release was determined by Fluo-4AM (5 μM) using confocal microscopy. Phase images are presented on the right. B, DDT_1 MF-2 cells were pretreated with vehicle or 20 μM BAPTA-AM for 30 min prior to the treatment with B-oligomer prior to determining NF-κB activity by electrophoretic mobility shift assays. Bottom, blots were quantitated by densitometric scanning and normalized to Oct-1. C, [^{3}H]DPCPX radioligand binding was performed on membrane preparations obtained from control cells and those treated with B-oligomer (1 nM), BAPTA-AM, or B-oligomer + BAPTA-AM. The data are presented as the mean ± S.E.M. of four independent experiments. Asterisks represent the statistical significant difference ($p < 0.05$). *, significant difference from control; **, significant difference from B-oligomer alone.

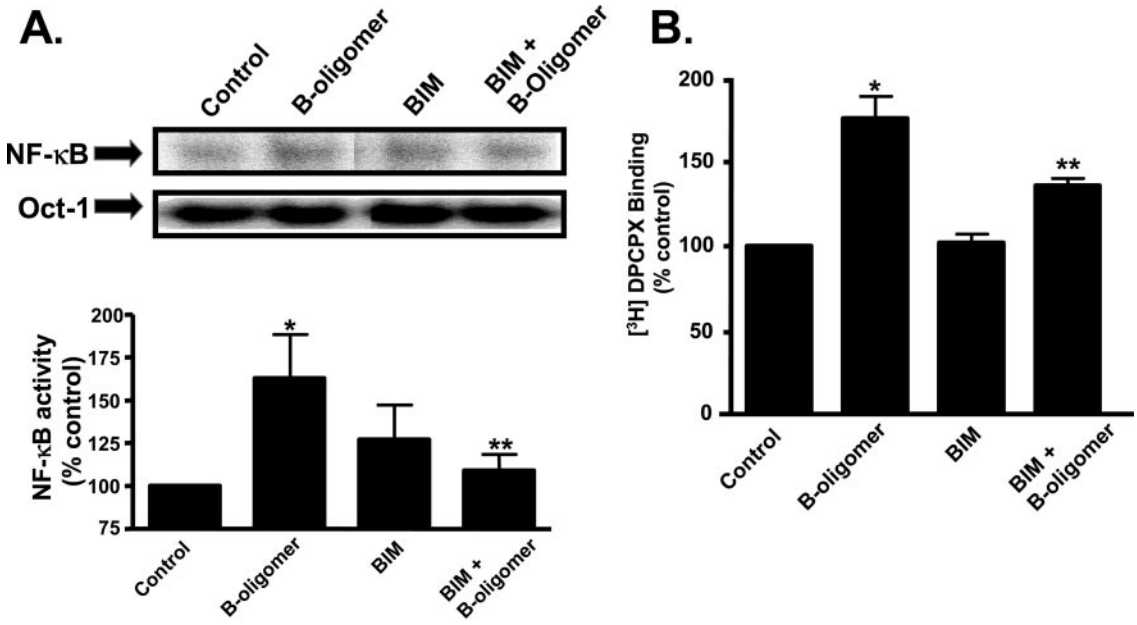

Fig. 7. Inhibition of protein kinase C attenuates the responses to B-oligomer. A, cells were pretreated with vehicle or with 1 μM BIM for 30 min, followed by administration of 1 nM B-oligomer. Nuclear preparations were obtained and used for electrophoretic mobility shift assays. Bottom, bar graphs show inhibition of B-oligomer stimulated NF-κB activation by BIM. Data are presented as the mean ± S.E.M. of three independent experiments. B, [^{3}H]DPCPX binding assays were performed on plasma membranes prepared from cells treated with vehicle, B-oligomer (1 nM), BIM (1 μM), or BIM + B-oligomer. Data represent mean ± S.E.M. of four independent experiments. *, $p < 0.05$ significant difference from control. **, $p < 0.05$ significant difference from B-oligomer.

gomer and other bacterial components could trigger induction of NF-κB-dependent genes. The induction of the A_1AR and other NF-κB regulated inflammatory proteins in the airway may contribute to the pathogenesis of the disease. Furthermore, activation of a similar NF-κB-dependent pathway by other bacterial toxins could trigger production of A_1AR and inflammatory cytokines and promote inflammation of the respiratory tract.

In summary, our data indicate that pertussis toxin uncouples the A_1AR from its coupling protein, leading to an increase in the affinity of the receptor for antagonist radioligand and induction of the A_1AR through activation of NF-κB. Although the increase in antagonist affinity is dependent on ADP ribosylation of G_i, the activation of NF-κB appears independent of this G protein modification. Induction of NF-κB-dependent genes following treatment of cultures with

pertussis toxin to effect ADP ribosylation could complicate the interpretation of experimental data.

References

Abebe W and Mustafa SJ (1998) A_1 adenosine receptor-mediated Ins (1,4,5)P3 generation in allergic rabbit airway smooth muscle. *Am J Physiol* **275:**L990–L997.

Asehnoune K, Strassheim D, Mitra S, Yeol Kim J, and Abraham E (2005) Involvement of PKC alpha/beta in TLR4 and TLR2 dependent activation of NF-kappaB. *Cell Signal* **17:**385–394.

Banga HS, Walker RK, Winberry LK, and Rittenhouse SE (1987) Pertussis toxin can activate human platelets: comparative effects of holotoxin and its ADP-ribosylating S1 subunit. *J Biol Chem* **262:**14871–14874.

Barrington WW, Jacobson KA, and Stiles GL (1989) Demonstration of distinct agonist and antagonist conformations of the A_1 adenosine receptor. *J Biol Chem* **264:**13157–13164.

Bradford MM (1976) A rapid and sensitive method for the quantitation of microgram quantities of protein utilizing the principle of protein-dye binding. *Anal Biochem* **72:**248–254.

Dickenson JM, Blank JL, and Hill SJ (1998) Human adenosine A_1 receptor and P2Y2-purinoceptor-mediated activation of the mitogen-activated protein kinase cascade in transfected CHO cells. *Br J Pharmacol* **124:**1491–1499.

Dunwiddie TV and Masino SA (2001) The role and regulation of adenosine in the central nervous system. *Annu Rev Neurosci* **24:**31–55.

Freissmuth M, Selzer E, and Schutz W (1991) Interactions of purified bovine brain A_1-adenosine receptors with G-proteins: reciprocal modulation of agonist and antagonist binding. *Biochem J* **275:**651–656.

Ghosh S, May MJ, and Kopp EB (1998) NF-kappa B and Rel proteins: evolutionarily conserved mediators of immune responses. *Annu Rev Immunol* **16:**225–260.

Gray LS, Huber KS, Gray MC, Hewlett EL, and Engelhard VH (1989) Pertussis toxin effects on T lymphocytes are mediated through CD3 and not by pertussis toxin catalyzed modification of a G protein. *J Immunol* **142:**1631–1638.

Green AJ (1987) Adenosine receptor down-regulation and insulin resistance following prolonged incubation of adipocytes with an A_1 adenosine receptor agonist. *J Biol Chem* **262:**15702–15707.

Iordanskiy S, Iordanskaya T, Quivy V, Van Lint C, and Bukrinsky M (2002) B-Oligomer of pertussis toxin inhibits HIV-1 LTR-driven transcription through suppression of NF-kappaB p65 subunit activity. *Virology* **302:**195–206.

Ishibashi Y and Nishikawa A (2003) Role of nuclear factor-kappa B in the regulation of intercellular adhesion molecule 1 after infection of human bronchial epithelial cells by *Bordetella pertussis*. *Microb Pathog* **35:**169–177.

Kaslow HR and Burns DL (1992) Pertussis toxin and target eukaryotic cells: binding, entry and activation. *FASEB J* **6:**2684–2690.

Kurachi Y, Nakajima T, and Sugimoto T (1986) On the mechanism of activation of muscarinic K^+ channels by adenosine in isolated atrial cells: involvement of GTP-binding proteins. *Pflueg Arch Eur J Physiol* **407:**264–274.

Lilienbaum A and Israel A (2003) From calcium to NF-kappa B signaling pathways in neurons. *Mol Cell Biol* **23:**2680–2698.

Longabaugh JP, Didsbury J, Spiegel A, and Stiles GL (1989) Modification of the rat adipocyte A_1 adenosine receptor-adenylate cyclase system during chronic exposure to an A_1 adenosine receptor agonist: alterations in the quantity of $G_{s\alpha}$ and $G_{i\alpha}$ are not associated with changes in their mRNAs. *Mol Pharmacol* **36:**681–688.

Lyakh LA, Koski GK, Telford W, Gress RE, Cohen PA, and Rice NR (2000) Bacterial lipopolysaccharide, TNF-alpha and calcium ionophore under serum-free conditions promote rapid dendritic cell-like differentiation in CD14+ monocytes through distinct pathways that activate NF-kappa B. *J Immunol* **165:**3647–3655.

Mattson MP and Camandola S (2001) NF-kappaB in neuronal plasticity and neurodegenerative disorders. *J Clin Investig* **107:**247–254.

Moscat J, Diaz-Meco MT, and Rennert P (2002) NF-kappaB activation by protein kinase C isoforms and B-cell function. *EMBO (Eur Mol Biol Organ) Rep* **4:**31–36.

Murayama T and Ui M (1983) Loss of the inhibitory function of the guanine nucleotide regulatory component of adenylate cyclase due to its ADP ribosylation by islet- activating protein, pertussis toxin, in adipocyte membranes. *J Biol Chem* **258:**3319–3326.

Nie Z, Mei Y, Ford M, Rybak L, Marcuzzi A, Ren H, Stiles GL, and Ramkumar V (1998) Oxidative stress increases A_1 adenosine receptor expression by activating nuclear factor kappa B. *Mol Pharmacol* **53:**663–669.

Ochiishi T, Chen L, Yukawa A, Saitoh Y, Sekino Y, Arai T, Nakata H, and Miyamoto H (1999) Cellular localization of adenosine A1 receptors in rat forebrain: immunohistochemical analysis using adenosine A1 receptor-specific monoclonal antibody. *J Comp Neurol* **411:**301–316.

Olah ME, Gallo-Rodriguez C, Jacobson KA, and Stiles GL (1994) ^{125}I-4-Aminobenzyl-5′-*N*-methylcarboxamidoadenosine, a high affinity radioligand for the rat A_3 adenosine receptor. *Mol Pharmacol* **45:**978–982.

Olah ME, Jacobson KA, and Stiles GL (1994) Role of the second extracellular loop of adenosine receptors in agonist and antagonist binding: analysis of chimeric A1/A3 adenosine receptors. *J Biol Chem* **269:**24692–24698.

Pahl HL and Baeuerle PA (1996) Activation of NF-kappa B by ER stress requires both Ca^{2+} and reactive oxygen intermediates as messengers. *FEBS Lett* **392:**129–136.

Palmer TM and Stiles GL (1995) Adenosine receptors. *Neuropharmacology* **34:**683–694.

Ramkumar V, Bumgarner JR, Jacobson KA, and Stiles GL (1988) Multiple components of the A_1 adenosine receptor-adenylate cyclase system are regulated in rat cerebral cortex by chronic caffeine ingestion. *J Clin Investig* **82:**242–247.

Ramkumar V, Olah ME, Jacobson KA, and Stiles GL (1991) Distinct pathways of desensitization of A_1 and A_2 adenosine receptors in DDT_1 MF-2 cells. *Mol Pharmacol* **40:**639–647.

Ramkumar V and Stiles GL (1988) Reciprocal modulation of agonist and antagonist binding to A_1 adenosine receptors by guanine nucleotides is mediated via a pertussis toxin-sensitive G protein. *J Pharmacol Exp Ther* **246:**1194–1200.

Ruiz A, Sanz JM, Gonzalez-Calero G, Fernandez M, Andres A, Cubero A, and Ros M (1996) Desensitization and internalization of adenosine A_1 receptors in rat brain by in vivo treatment with R-PIA: involvement of coated vesicles. *Biochim Biophys Acta* **1310:**168–174.

Saijo K, Mecklenbrauker I, Santana A, Leitger M, Schmedt C, and Tarakhovsky A (2002) Protein kinase C beta controls nuclear factor kappaB activation in B cells through selective regulation of the IkappaB kinase alpha. *J Exp Med* **195:**1647–1652.

Sen CK, Roy S, and Packer L (1996) Involvement of intracellular Ca^{2+} in oxidant-induced NF-kappa B activation. *FEBS Lett* **385:**58–62.

Shryock J, Patel A, Belardinelli L, and Linden J (1989) Down-regulation and desensitization of A_1-adenosine receptor in embryonic chick heart. *Am J Physiol* **256:**H321–H327.

Sindt KA, Hewlett EL, Redpath GT, Rappuoli R, Gray LS, and Vandenberg SR (1994) Pertussis toxin activates platelets through an interaction with platelet glycoprotein Ib. *Infect Immun* **62:**3108–3114.

Sperelakis N (1987) Regulation of calcium slow channels of cardiac and smooth muscles by adenine nucleotides. *Prog Clin Biol Res* **230:**35–193.

Stiles GL (1991) Adenosine receptors. *J Biol Chem* **267:**6451–6454.

Sun SC, Ganchi PA, Ballard DW, and Greene WC (1993) NF-κB controls expression of inhibitor IκBα: evidence for an inducible autoregulatory pathway. *Science (Wash DC)* **259:**1912–1915.

Tonon S, Goriely S, Aksoy E, Pradier O, Del Giudice G, Trannoy E, Willems F, Goldman M, and De Wit D (2002) *Bordetella pertussis* toxin induces the release of inflammatory cytokines and dendritic cell activation in whole blood: impaired responses in human newborns. *Eur J Immunol* **32:**3118–3125.

Wong WS and Rosoff PM (1996) Pharmacology of pertussis toxin B-oligomer. *Can J Physiol Pharmacol* **74:**559–564.

Address correspondence to: Dr. Vickram Ramkumar, Southern Illinois University School of Medicine, P.O. Box 19629, Springfield, IL 62794-9629. E-mail: vramkumar@siumed.edu